Biogeosciences, 11, 2295–2308, 2014
www.biogeosciences.net/11/2295/2014/
doi:10.5194/bg-11-2295-2014

Biogeosciences Open Access

Environmental controls on the *Emiliania huxleyi* calcite mass

M. T. Horigome[1], P. Ziveri[1,2], M. Grelaud[1], K.-H. Baumann[3], G. Marino[1,*], and P. G. Mortyn[1,4]

[1]Institute of Environmental Science and Technology, Universitat Autònoma de Barcelona, Bellaterra 08193, Spain
[2]Earth & Climate Cluster, Department of Earth Sciences, FALW, Vrije Universiteit Amsterdam, FALW, HV1081 Amsterdam, the Netherlands
[3]Fachbereich Geowissenschaften, Universität Bremen, Postfach 330440, 28334 Bremen, Germany
[4]Department of Geography, Universitat Autònoma de Barcelona, Bellaterra 08193, Spain
[*]now at: Research School of Earth Sciences, The Australian National University, Canberra 0200, Australia

Correspondence to: P. Ziveri (patrizia.ziveri@uab.es)

Received: 28 March 2013 – Published in Biogeosciences Discuss.: 10 June 2013
Revised: 3 March 2014 – Accepted: 5 March 2014 – Published: 24 April 2014

Abstract. Although ocean acidification is expected to impact (bio) calcification by decreasing the seawater carbonate ion concentration, [CO_3^{2-}], there is evidence of nonuniform response of marine calcifying plankton to low seawater [CO_3^{2-}]. This raises questions about the role of environmental factors other than acidification and about the complex physiological responses behind calcification. Here we investigate the synergistic effect of multiple environmental parameters, including seawater temperature, nutrient (nitrate and phosphate) availability, and carbonate chemistry on the coccolith calcite mass of the cosmopolitan coccolithophore *Emiliania huxleyi*, the most abundant species in the world ocean. We use a suite of surface (late Holocene) sediment samples from the South Atlantic and southwestern Indian Ocean taken from depths lying above the modern lysocline (with the exception of eight samples that are located at or below the lysocline). The coccolith calcite mass in our results presents a latitudinal distribution pattern that mimics the main oceanographic features, thereby pointing to the potential importance of seawater nutrient availability (phosphate and nitrate) and carbonate chemistry (pH and pCO_2) in determining coccolith mass by affecting primary calcification and/or the geographic distribution of *E. huxleyi* morphotypes. Our study highlights the importance of evaluating the combined effect of several environmental stressors on calcifying organisms to project their physiological response(s) in a high-CO_2 world and improve interpretation of paleorecords.

1 Introduction

Coccolithophores are an abundant marine phytoplankton group that plays a significant role in both the marine food web and the carbon cycle (Young, 1994), comprising an important sedimentary carbon reservoir (Berger, 1976; Ridgwell and Zeebe, 2005). They are responsible for the photosynthetic fixation of inorganic carbon, regulating the particulate inorganic : organic carbon ratio and a large portion of the calcium carbonate ($CaCO_3$) production (Raven et al., 2005). The relative strength of photosynthesis and calcification at the surface ocean determines the biologically mediated exchange of carbon dioxide (CO_2) between the oceanic and atmospheric carbon reservoirs (Sigman et al., 2010), making quantification of these two processes central to our understanding of the dynamics of the global carbon cycle. The export of carbon and $CaCO_3$ to the seafloor enhances the ocean's capability to buffer the rise of atmospheric CO_2 concentrations (Van Cappellen, 2003; Ploug et al., 2008; Doney et al., 2009). The coccolithophore calcite plates (coccoliths) are in fact a major source of calcite to the calcareous deep-sea oozes that cover almost half of the global oceanic floor (Berger, 1976; Ridgwell and Zeebe, 2005). Despite the role of coccolithophores in the marine carbon cycle, the environmental factors modulating their calcification remain debated. In order to investigate the controlling factors of coccolithophore calcification, research has centered on their variability in mass and size (Beaufort and Heussner, 1999; Young and Ziveri, 2000) in different types of experimental and field observational settings. Several environmental

parameters have been examined (Broerse et al., 2000; Beaufort et al., 2008; Henderiks et al., 2012), such as light (Paasche, 2001), nutrient availability (Winter et al., 1994; Båtvik et al., 1997; Paasche, 1998; Müller et al., 2012), calcification temperature (Bollmann et al., 2002; Ziveri et al., 2004; Boeckel et al., 2006), salinity (Bollmann and Herrle, 2007; Bollmann et al., 2009; Fielding et al., 2009), and carbonate chemistry (Iglesias-Rodriguez et al., 2008; Langer et al., 2009; de Bodt et al., 2010; Müller et al., 2010; Barcelos e Ramos et al., 2010; Beaufort et al., 2011; Bach et al., 2012).

Ongoing ocean acidification (due to the oceanic uptake of the anthropogenic carbon from the atmosphere) is expected to impact marine calcifying organisms, such as coccolithophores (Van Cappellen, 2003; Feely et al., 2004; Delille et al., 2005; Fabry et al., 2008). Increasing partial pressures of CO_2 in the ocean (pCO_2) leads to a decrease of $[CO_3^{2-}]$ and to a decline of the calcite saturation state of seawater (Zeebe and Wolf-Gladrow, 2001; Raven et al., 2005; Fabry et al., 2008), which has been proposed as an important factor in the reduction of coccolith mass (Riebesell et al., 2000; Delille et al., 2005; Langer et al., 2009; Beaufort et al., 2011). However, complementary evidence points to a nonuniform response of calcification to high CO_2 (cf. Langer et al., 2006; Iglesias-Rodriguez et al., 2008; Riebesell et al., 2008; Doney et al., 2009), casting doubts on the notion that $[CO_3^{2-}]$ is the prime (and sole) controlling factor of (bio)calcification. In order to advance our understanding of the role played by different physicochemical properties of seawater on coccolithophore calcification, we examined a widely distributed suite of surface sediment samples taken along oceanic transects characterized by steep surface ocean environmental gradients, such as the South Atlantic and southwestern Indian oceans, the Agulhas System, and the subantarctic sector of the Southern Ocean. Most of the samples were selected from coring sites lying above the depth of the modern lysocline (Boeckel and Baumann, 2008). This reduces (or even precludes) the post-depositional effects (dissolution) on the coccolith calcite preservation, thereby allowing recognition of the surface ocean environmental factors influencing the coccolith mass. Significant calcium carbonate dissolution is expected to begin firstly below 5000 m in the deep Guinea and Angola basins and below 4400 m in the Cape Basin (Volbers and Henrich, 2002), although ultrastructural breakdown of foraminifera shells already begins at shallower depths. However, only eight of the studied samples are from a depth close to or slightly below 4400 m and only two of them are from $>$ 4500 m (Table 1). Therefore, the preservation of the selected samples is mostly good and has been documented by scanning electron microscope (SEM) in earlier work (e.g., Boeckel et al., 2006: Boeckel and Baumann, 2008).

Hence, the new surface sediment data set presented here has the potential to elucidate the influence of multiple environmental parameters at the ocean surface (temperature, salinity, nutrients, pH, $[CO_3^{2-}]$, and pCO_2) on the coccolith mass of the most common living, blooming coccolithophore species *Emiliania huxleyi*. The majority of studies employ culture experiments to test the response on the calcite mass of *E. huxleyi* to changing environmental parameters (Langer et al., 2006; Iglesias-Rodriguez et al., 2008; Riebesell et al., 2008; Bach et al., 2012; Müller et al., 2012). Although surface sediments may constrain variations in the individual environmental parameters less precisely than culture studies they allow evaluating the combined effect of a full suite of environmental property gradients on the (*E. huxleyi*) coccolith mass variations. In addition, surface sediment studies apply methodological protocols (and assumptions) that are identical to down-core studies, thereby providing an ideal format from which to interpret past coccolith mass changes, e.g., across glacial–interglacial changes in atmospheric CO_2 concentrations (e.g., Monnin et al., 2001; Lüthi et al., 2008) and seawater carbonate chemistry (e.g., Hönisch and Hemming, 2005; Foster, 2008).

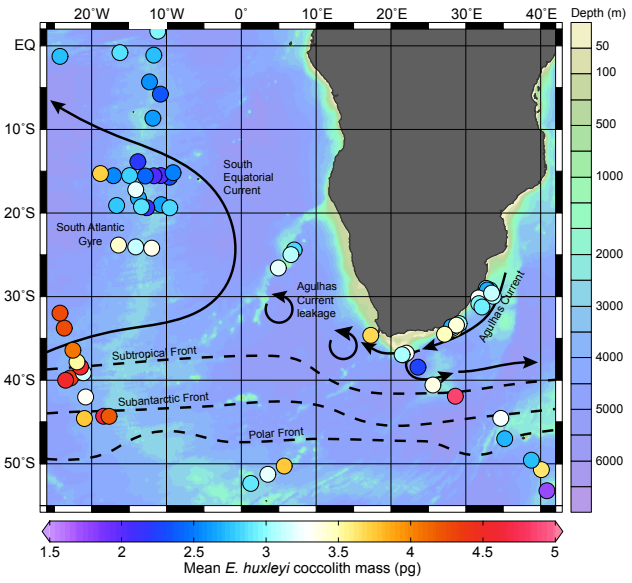

Fig. 1. Distribution map of the studied sites (circles). The color of the symbols (scale at the bottom) refers to the averaged mass of *E. huxleyi* coccoliths measured at the different sites. The bathymetry is given by the scale on the right side. The surface hydrography is depicted by the black arrows and the main fronts by the dotted lines.

1.1 Oceanographic setting

The South Atlantic, the Agulhas System, and the Southern Ocean are characterized by strong gradients in surface water properties, such as temperature, salinity, and nutrient concentration (Mizuki et al., 1994; Lutjeharms, 2006). This region is marked by the strongest physicochemical gradients in the entire global ocean, with temperature changes of approximately 13 °C within 12° of latitude. The surface circulation is driven by the atmospheric pressure gradients (winds),

Table 1. Sample information. The sedimentation rates or the maximum age of samples were extracted from (1) Mollenhauer et al. (2004), (2) Jonkers et al. (2012), (3) Martínez-Méndez, et al. (2010). The asterisk (*) shows that the sedimentation rate was calculated for that specific core, otherwise it has been estimated from sedimentation rates calculated for nearby cores.

Sample	Cruise	Year	Latitude	Longitude	Depth (m)	Sed. Rate (cm ka^{-1})	Max. age (yr)	*E. huxleyi* mass (pg)	Noëlaerhabdaceae mass (pg)
1112-3	M9-4	1989	06° 18′23″ S	11° 14′33″ W	3128	2.8*$_{(1)}$	357	2.35 ± 0.59	1.95 ± 1.11
1203-2	M12-1	1990	26° 55′00″ S	05° 02′00″ E	2395	1.5*$_{(1)}$	667	3.21 ± 0.91	12.36 ± 3.07
1208-1	M12-1	1990	24° 49′00″ S	07° 11′00″ E	2971	3.2$_{(1)}$	313	2.83 ± 0.70	11.36 ± 3.22
1217-1	M12-1	1990	25° 35′00″ S	07° 13′00″ E	2007	2.5$_{(1)}$	400	3.08 ± 0.72	8.57 ± 2.96
1403-2	M16-1	1991	01° 20′23″ S	12° 11′17″ W	3692	3.8$_{(1)}$	265	2.72 ± 0.73	9.95 ± 3.13
1405-7	M16-1	1991	02° 09′00″ N	11° 13′33″ W	4393	3$_{(1)}$	333	2.94 ± 0.86	10.75 ± 4.70
1413-2	M16-1	1991	16° 07′50″ S	09° 46′07″ W	3785	1.1*$_{(1)}$	909	2.28 ± 0.46	8.05 ± 1.86
1414-2	M16-1	1991	15° 53′23″ S	11° 13′23″ W	3605	1.7*$_{(1)}$	588	2.02 ± 0.50	13.13 ± 3.06
1415-1	M16-1	1991	15° 53′00″ S	11° 58′23″ W	3116	1.2*$_{(1)}$	833	2.02 ± 0.62	9.30 ± 2.65
1417-1	M16-1	1991	15° 54′00″ S	13° 11′07″ W	2845	2.5*$_{(1)}$	400	2.40 ± 0.67	3.93 ± 1.69
1418-1	M16-1	1991	15° 53′33″ S	15° 28′50″ W	3524	1.3$_{(1)}$	769	2.80 ± 0.60	10.00 ± 3.03
1419-1	M16-1	1991	15° 54′23″ S	17° 07′00″ W	4024	1.8$_{(1)}$	556	2.53 ± 0.60	9.14 ± 2.80
1420-1	M16-1	1991	15° 35′33″ S	19° 09′07″ W	4587	1.8$_{(1)}$	556	3.72 ± 0.73	10.04 ± 3.57
1901-1	So84	1993	01° 22′07″ S	16° 24′20″ W	2879	3.9$_{(1)}$	256	2.84 ± 0.69	13.81 ± 2.78
1902-3	So84	1993	04° 38′17″ S	12° 20′23″ W	2744	3.5$_{(1)}$	286	2.55 ± 0.67	0.93 ± 1.25
1903-1	So84	1993	09° 08′05″ S	12° 24′33″ W	3161	2.2$_{(1)}$	455	2.61 ± 0.58	13.08 ± 3.48
1904-1	So84	1993	14° 28′33″ S	14° 21′50″ W	3041	1.3$_{(1)}$	769	2.17 ± 0.52	8.73 ± 2.82
1905-1	So84	1993	17° 14′33″ S	14° 39′07″ W	2972	1.8$_{(1)}$	556	3.20 ± 0.73	10.91 ± 3.51
1906-1	So84	1993	18° 22′00″ S	14° 15′17″ W	2843	2.3$_{(1)}$	444	2.67 ± 0.57	4.34 ± 2.03
1907-1	So84	1993	15° 13′07″ S	09° 09′23″ W	3382	1.1$_{(1)}$	909	2.52 ± 0.58	7.66 ± 2.16
2213-1	M23-2	1994	01° 26′50″ S	24° 15′33″ W	4323	2.3$_{(1)}$	435	2.72 ± 0.54	7.08 ± 2.10
5112-5	M41-3	1998	24° 22′50″ S	16° 26′23″ W	3841	3.6$_{(1)}$	278	3.41 ± 0.58	9.25 ± 3.13
5115-2	M41-3	1998	24° 14′33″ S	14° 04′33″ W	3291	3.6$_{(1)}$	278	3.09 ± 0.59	9.54 ± 2.54
5121-2	M41-3	1998	24° 18′33″ S	12° 02′17″ W	3486	3.6$_{(1)}$	278	3.32 ± 0.61	8.45 ± 3.05
5130-1	M41-3	1998	19° 40′33″ S	09° 46′23″ W	3166	2.2$_{(1)}$	455	2.82 ± 0.59	8.97 ± 2.59
5134-1	M41-3	1998	19° 04′50″ S	11° 08′33″ W	3411	2.2$_{(1)}$	455	2.62 ± 0.58	5.10 ± 1.57
5136-2	M41-3	1998	19° 37′00″ S	13° 07′00″ W	3227	2.2$_{(1)}$	455	2.12 ± 0.53	7.53 ± 2.10
5137-1	M41-3	1998	19° 29′17″ S	13° 45′33″ W	3502	2.25$_{(1)}$	444	2.84 ± 0.61	12.47 ± 3.23
5140-3	M41-3	1998	19° 05′17″ S	17° 01′33″ W	3660	2.3$_{(1)}$	435	2.77 ± 0.46	1.01 ± 0.98
6402-9	M46/4	2001	40° 14′27″ S	23° 16′05″ W	3878	3.3$_{(1)}$	303	4.34 ± 0.63	12.50 ± 3.65
6403-4	M46/4	2001	40° 01′33″ S	23° 36′52″ W	4226	3.3$_{(1)}$	303	4.53 ± 0.77	11.68 ± 3.81
6406-1	M46/4	2001	42° 00′03″ S	21° 18′40″ W	3514	6.7$_{(1)}$	149	3.31 ± 0.62	11.51 ± 3.93
6410-1	M46/4	2001	44° 52′08″ S	21° 30′00″ W	4038	6.7$_{(1)}$	149	3.74 ± 0.62	10.91 ± 3.35
6411-4	M46/4	2001	44° 36′33″ S	18° 35′20″ W	3893	4.4$_{(1)}$	227	4.63 ± 0.69	10.75 ± 3.79
6412-1	M46/4	2001	44° 25′40″ S	18° 05′07″ W	3475	4.4$_{(1)}$	227	4.17 ± 0.59	13.64 ± 3.64
6417-2	M46/4	2001	39° 09′33″ S	21° 04′17″ W	4024	3.3$_{(1)}$	303	3.15 ± 0.63	6.21 ± 2.63
6418-3	M46/4	2001	38° 43′05″ S	21° 53′50″ W	4126	3.3$_{(1)}$	303	4.56 ± 0.66	9.05 ± 3.89
6419-1	M46/4	2001	38° 17′40″ S	22° 26′42″ W	3568	3.3$_{(1)}$	303	3.54 ± 0.63	5.00 ± 2.41
6421-2	M46/4	2001	36° 45′23″ S	22° 44′50″ W	4220	3.3$_{(1)}$	303	4.06 ± 0.59	11.21 ± 3.91
6425-1	M46/4	2001	34° 22′00″ S	23° 59′15″ W	4352	0.6$_{(1)}$	1667	4.25 ± 0.62	10.37 ± 4.52
6429-1	M46/4	2001	32° 35′00″ S	24° 25′23″ W	4335	0.6$_{(1)}$	1667	4.25 ± 0.64	10.42 ± 3.41
ANT2557-2	ANTXI-4	1994	37° 35′00″ S	22° 18′00″ E	3371			3.25 ± 0.55	9.70 ± 3.77
ANT2558-1	ANTXI-4	1994	38° 49′00″ S	24° 06′00″ E	5262			2.24 ± 0.55	4.81 ± 2.24
ANT2560-3	ANTXI-4	1994	40° 55′00″ S	25° 57′00″ E	2641			3.36 ± 0.59	9.39 ± 3.39
ANT2561-1	ANTXI-4	1994	42° 26′00″ S	28° 57′00″ E	4471			4.85 ± 0.71	10.11 ± 3.34
ANT2563-3	ANTXI-4	1994	44° 56′00″ S	35° 19′00″ E	3515			3.27 ± 0.52	11.53 ± 3.98
ANT2565-2	ANTXI-4	1994	47° 00′00″ S	35° 21′00″ E	3682			2.70 ± 0.54	9.16 ± 2.23
ANT2568-3	ANTXI-4	1994	50° 21′00″ S	06° 16′00″ E	3791	1.2$_{(1)}$	833	3.74 ± 0.58	9.18 ± 2.80
ANT2569-1	ANTXI-4	1994	51° 26′00″ S	03° 59′00″ E	3333	1.2$_{(1)}$	833	3.19 ± 0.65	8.55 ± 2.34
ANT2570-1	ANTXI-4	1994	52° 33′00″ S	01° 28′00″ E	2575	1.2$_{(1)}$	833	2.89 ± 0.61	7.18 ± 3.28
ANT2606-3	ANTXI-4	1994	53° 22′00″ S	41° 27′00″ E	2552			1.73 ± 0.43	6.01 ± 3.04
ANT2610-1	ANTXI-4	1994	51° 07′50″ S	40° 12′00″ E	3584			3.62 ± 0.62	9.46 ± 3.36
ANT2611-2	ANTXI-4	1994	49° 47′00″ S	39° 20′00″ E	4449			2.73 ± 0.66	7.00 ± 2.10
CD154 01-01K	CD154	2003/04	29° 29′10″ S	33° 14′40″ E	1997		< 150*$_{(2)}$	2.84 ± 0.57	9.93 ± 3.93
CD154 02-03K	CD154	2003/04	29° 06′40″ S	33° 17′30″ E	1626		< 150*$_{(2)}$	2.90 ± 0.55	9.50 ± 3.57
CD154 03-05K	CD154	2003/04	29° 12′10″ S	33° 29′20″E	1747		< 150*$_{(2)}$	2.67 ± 0.59	9.92 ± 3.35
CD154 05-07K	CD154	2003/04	30° 33′40″ S	34° 21′50″ E	1850		<150*$_{(2)}$	3.06 ± 0.58	10.44 ± 5.32
CD154 07-07PK	CD154	2003/04	30° 13′20″ S	32° 10′10″ E	1017			3.31 ± 0.55	9.94 ± 3.99
CD154 09-09K	CD154	2003/04	31° 23′50′′S	32° 14′20″ E	2986			2.95 ± 0.59	9.82 ± 3.67
CD154 10-10K	CD154	2003/04	31° 17′00″ S	32° 15′00″ E	3074		<150*$_{(2)}$	2.93 ± 0.57	9.04 ± 4.03
CD154 04-06K	CD154	2003/04	29° 59′00″ S	33° 44′00″ E	2469			3.09 ± 0.59	9.72 ± 3.69
CD154 15-13K	CD154	2003/04	34° 09′10″ S	28° 25′10″ E	3145			3.53 ± 0.66	10.01 ± 3.67
CD154 15-14K	CD154	2003/04	34° 13′10″ S	28° 20′30″ E	3236			3.15 ± 0.54	9.83 ± 4.28
CD154 16-15K	CD154	2003/04	34° 10′10″ S	28° 24′30″ E	3166			2.69 ± 0.55	11.26 ± 3.36
CD154 17-17K	CD154	2003/04	33° 27′30″ S	29° 12′20″ E	3333			3.01 ± 0.58	9.87 ± 4.36
CD154 18-18K	CD154	2003/04	33° 31′20″ S	28° 25′00″ E	3037			3.39 ± 0.52	10.65 ± 3.71
CD154 20-20K	CD154	2003/04	34° 45′00″ S	27° 15′20″ E	3512			3.44 ± 0.60	10.08 ± 4.03
CD154 23-24K	CD154	2003/04	37° 20′40″ S	22° 01′00″ E	3173			3.30 ± 0.52	10.24 ± 3.12
CD154 24-25K	CD154	2003/04	37° 36′20″ S	21° 55′30″ E	3417			3.03 ± 0.57	11.23 ± 2.85
MD02-2594	MD128	2003	35° 11′00″ S	17° 34′00″ E	2440	17.9*$_{(3)}$	56	3.66 ± 0.66	10.86 ± 3.03

with the subtropical regions controlled by an anticyclonic regime and the higher latitude portion governed by westerly winds and eastward-directed Antarctic Circumpolar Current (ACC) (e.g., Toggweiler et al., 2006; Rintoul, 2009). The ACC is a complex structure with the demarcation of three main fronts, the Subtropical Front (STF), the Subantarctic Front (SAF) and the Polar Front (PF) (Fig. 1), each associated with an intense cross-stream gradient in temperature, salinity and (biogeo)chemical properties (Orsi et al., 1995; Rintoul, 2009). The fronts of the ACC define thermal and biological boundaries, representing a wide latitudinal band ranging from subtropical nutrient-depleted water to nutrient-rich polar waters that enhance the productivity (Orsi et al., 1995; Banse, 1996). They create biogeographic zones with a dominance of coccolithophores and small zooplankton at the north of the SAF (Popp et al., 1999; Rintoul, 2009). The higher biological productivity near fronts is due to advection of nutrients by the currents and injection of nutrient-rich waters from below (Sokolov and Rintoul, 2007; Rintoul, 2009). Another important circulation feature in the study area is the South Equatorial Current (SEC), a cross-equatorial surface current that transports waters from the South Atlantic Gyre to the North Atlantic Ocean (Peterson and Stramma, 1991). The study area also comprises the Agulhas Current, a strong western-boundary current that reaches the southern tip of Africa, where it retroflects, leaking warm and saline waters into the South Atlantic (Lutjeharms, 2006).

2 Materials and methods

Coccolith calcite plates of coccolithophores are formed in the upper photic zone and are eventually exported to the sea floor via macroaggregates and fecal pellets (Honjo, 1975; Young, 1994: Fischer and Karakas, 2009). Such particles contain high amounts of coccoliths and can reach sinking rates of up to several hundred meters per day (Ploug et al., 2008), allowing comparison between the coccoliths retrieved in the surface sediments and the properties of the surface waters just above them.

The studied region has up to 80 % of the carbonate sediment originating from coccolith calcite (Baumann et al., 2004; Frenz et al., 2005). We assessed the carbonate mass and distal shield length of individual coccolith specimens of the family Noëlaerhabdaceae (including *E. huxleyi*) in 70 surface sediment samples taken in the South Atlantic and southwestern Indian oceans. A total of 62 samples were retrieved above the modern lysocline (Volbers and Henrich, 2002) from water depths ranging between $\sim$ 1000 and $\sim$ 4400 m; only 8 samples were from deeper depths (up to 5260 m) (Fig. 1). The samples were obtained during several cruises from 1989 to 2004 and are listed in Table 1. Generally, the uppermost centimeter of the sediment column was sampled, with the exception of two samples from cruise CD154, for which the interval of 1–2 cm below the surface was selected.

Ages of the samples range between modern and late Holocene (Baumann et al., 2004) although there is no direct age control on many of the samples analyzed. The sedimentary data that we generated is then directly comparable with preindustrial surface ocean physicochemical properties. For example, samples with available ^{14}C and/or ^{210}Pb data (i.e., 1413-2, 1414-2, 1415-1, 1417-1, CD154-01-01K, CD154-02-03K, CD154-03-05K, CD154-05-07K, CD154-10-10K, and MD02-2594) are proven to have modern- to late-Holocene ages (Martinez-Mendez et al., 2010; Jonkers et al., 2012; Mollenhauer et al., 2004). In addition, the basic evidence that the remaining samples from the wider South Atlantic region are at least of Holocene age (and not older) comes from nearby ^{14}C- and/or ^{210}Pb-dated core tops (Mollenhauer, 2002; Mollenhauer et al., 2003, 2004, 2006, 2007), and from a number of investigated sediment cores from the entire study region, all yielding Holocene ages at the top (e.g., various articles in Wefer et al., 2004). Despite this large variability in age, the available data collectively rule out the possibility of "contamination" by sediments of glacial age, when physicochemical conditions in both the surface- and deep ocean were indeed substantially different from the modern Holocene (e.g., Hönisch and Hemming, 2005; Foster, 2008; Yu et al., 2010). In Table 1, we provide the information on sedimentation rates (or their estimation from nearby records) as available in the published literature. Since the age of the samples analyzed here is (late) Holocene to preindustrial, we corrected the modern values of the carbonate system parameters for the influence of anthropogenic CO_2 (Sabine et al., 2004) (see Sect. 3.2).

2.1 Calibration slides and coccolith mass estimation

Smear slides of surface sediment samples were prepared following standard procedures (e.g., Bown and Young, 1998). We used a Leica DM6000B cross-polarized light microscope with $\times$ 1000 magnification fitted with a SPOT Insight Camera. For each sample, we took on average 50 pictures that were analyzed with SYRACO, an automated system of coccolith recognition (SYstème de Reconnaissance Automatique de COccolithes) that is able to make the distinction between the different species composing the assemblages (Dollfus and Beaufort, 1999; Beaufort and Dollfus, 2004). Although a morphological study was performed on the coccoliths belonging to the family Noëlaerhabdaceae (including the genera *Emiliania*, *Gephyrocapsa*, and *Reticulofenestra*), we specifically focused on the species *E. huxleyi*. The coccolith length in relation to the distal shield was converted from pixels to micrometers: the pictures having a resolution of 832 pixels $\times$ 832 pixels, 1 pixel corresponding to $\sim$ 0.15 µm. The masses of single coccoliths were estimated using the method developed by Beaufort (2005) based on the brightness properties of calcite particles (with a thickness <1.55 µm) when viewed in cross-polarized light.

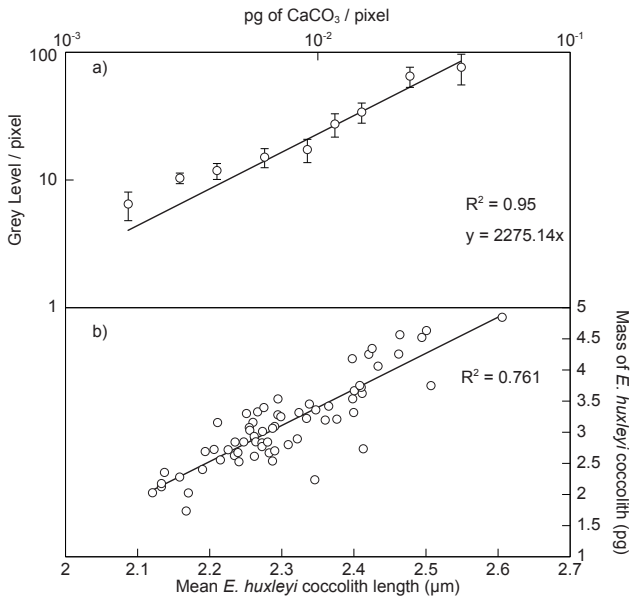

Fig. 2. Method calibration and validation. **(a)** Relation between the mass of calcite and the average GL values. The x and y axes are both on a logarithmic scale. The regression line (black) is forced to the axis origin. The vertical error bars give the 2σ standard deviation **(b)** *E. huxleyi* coccolith length versus mass, with black line indicating the linear regression.

A total of nine calibration slides were prepared with known amounts of pure crystalline calcite particles, the same as used by Beaufort (2005). Those particles have an elongated shape with a length ranging from 1 to 5 µm and a thickness compatible with our purpose (< 1.55 µm). We used cellulose acetate membrane filters and a low-pressure vacuum pump to have an even particle distribution. A total of 100 pictures in grey level (GL) were taken for each calibration slide. Then, for each amount of calcite, we estimated the averaged GL for 1 pixel and compared it to the averaged mass of calcite for 1 pixel (Fig. 2a). It was then possible to calculate the mass of a single coccolith as follows:

$$M_{\mathrm{coc}} = \sum \mathrm{GL}_{\mathrm{coc}}/2275.14, \quad (1)$$

where M_{coc} is the mass of a coccolith, expressed in pg, and $\Sigma\mathrm{GL}_{\mathrm{coc}}$ is the sum of the GL composing the picture of this coccolith. The constant 2275.14 is the slope of the linear regression presented in Fig. 2a. The correlation between length and mass is shown in Fig. 2b.

The luminosity of the microscope plays a significant role in both methods (SYRACO and calcite mass estimation), since the measurements are based on the brightness of the coccoliths when viewed in cross-polarized light. The luminosity is routinely checked in order to prevent any change due to the aging of the light bulb (see Supplement). Then the luminosity of the microscope was adjusted depending of the type of sample. Indeed a higher luminosity is required for slides containing a portion of membrane filter while a lower luminosity is needed for smear slides. For more details about those settings, refer to Fig. S1 of the Supplement.

2.2 Environmental parameters

The environmental parameters discussed in this study were extracted from existing databases. The temperature and salinity data were retrieved from the World Ocean Atlas (WOA) 2009 (http://www.nodc.noaa.gov/OC5/WOA09/pr_woa09.html), while the concentrations of phosphate and nitrate were retrieved from the WOCE (World Ocean Circulation Experiment) Global Hydrographic Climatology database (Gouretski and Koltermann, 2004). The modern total alkalinity and total dissolved carbon data were extracted from the global alkalinity and total dissolved carbon estimates database (Goyet et al., 2000). We used the anthropogenic CO_2 data set from the GLODAP (Global Ocean Data Analysis Project) website (http://cdiac.esd.ornl.gov/oceans/glodap/index.html) to correct the total dissolved carbon values from the anthropogenic "footprint"; the values of the anthropogenic CO_2 were removed from those of the total dissolved carbon. Finally, we used the total alkalinity and the corrected total dissolved carbon to calculate the pH, the $[CO_3^{2-}]$, and the pCO_2 in seawater, using CO2sys (Lewis and Wallace, 1998). The data sets were processed with Ocean Data View (ODV, Schlitzer, 2009) and the values closest to the sample locations were extracted at different depths (0, 10, 20, 30, 40 and 50 m) and averaged between 0 and 50 m in order to characterize the upper water column. Finally the mean annual data of chlorophyll *a* (Chl *a*) concentration, which is used here as an indicator of the surface productivity, was extracted from the Seaviewing Wide Field-of-view Sensor (SeaWiFS) project. The Chl *a* data are distributed as a Level-3 Binned file product (BIN), reprocessing no. 5, October 2011 (Feldman and McClain, 2011). The annual composites were downloaded from the http://oceancolor.gsfc.nasa.gov/ website in Hierarchical Data Format (HDF). The images have a resolution of 9 km^2 (4320″2160 pixels) and were analyzed using Sea-WiFS Data Analysis System (SeaDAS; Baith et al., 2001). Information was extracted from the pixels closest to the location of the surface sediment sample sites. A surface distribution map of all the environmental parameters discussed in this study is presented in Fig. S2 of the Supplement. These parameters were selected since they are important in controlling coccolith ecology and calcification. Even if the coccolithophore production layer depth in the open ocean expands towards the Equator, most *E. huxleyi* production occurs in the surface (Okada and Honjo, 1973; Okada and McIntyre, 1977). We therefore use environmental parameters extrapolated from the upper 50 m.

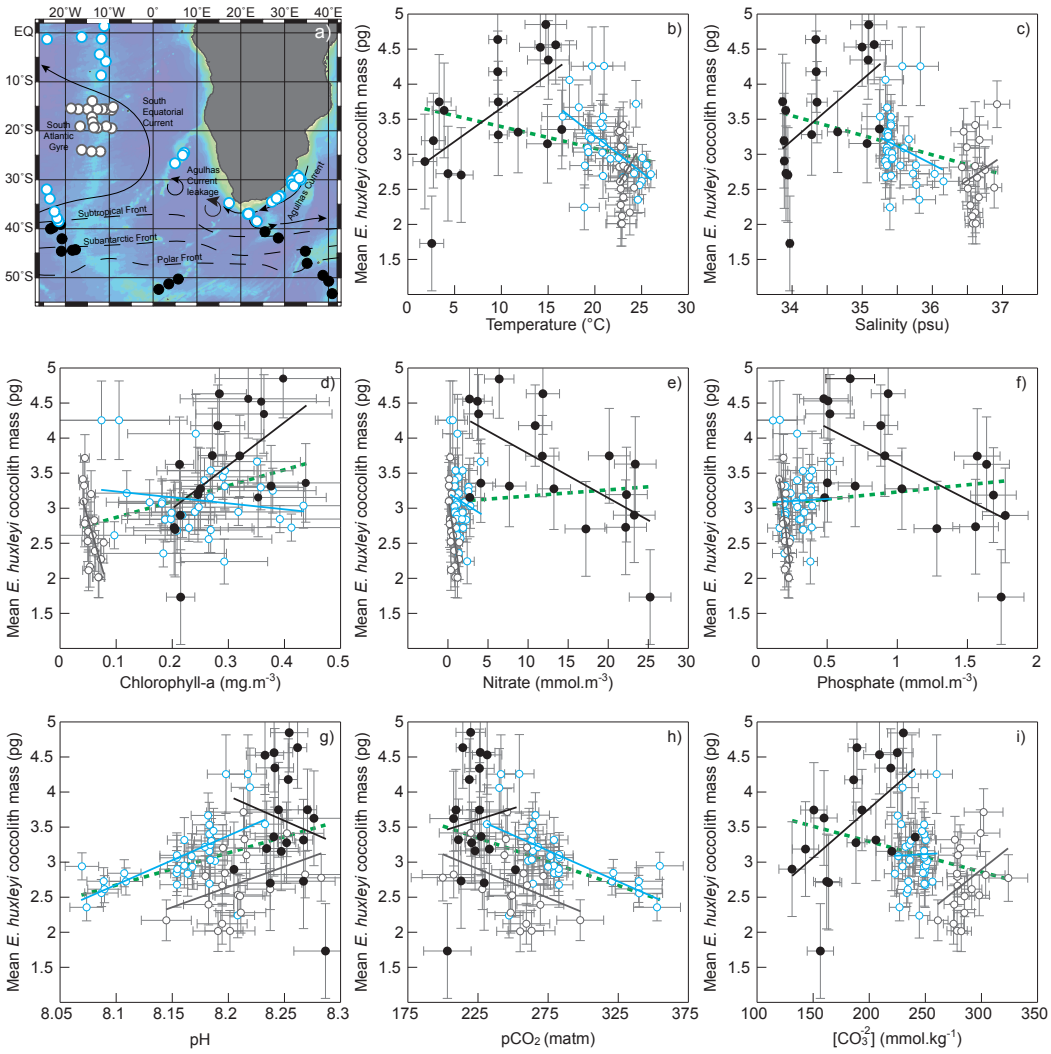

Fig. 3. (a) Distribution map of the samples according to the results of the cluster analysis performed of the environmental parameters (cluster #1 blue circles, cluster #2 open circles and cluster #3 filled black circles). For more details concerning the cluster analysis, see Fig. S2 of the Supplement. **(b)** – **(i)** Relations between the mass of *E. huxleyi* coccoliths and the environmental parameters for the three clusters (the symbols are the same as in **(a)**): **(b)** temperature, **(c)** salinity, **(d)** chlorophyll *a*, **(e)** nitrate, **(f)** phosphate, **(g)** pH, **(h)** pCO_2 and **(i)** $[CO_3^{2-}]$. The error bars give the 1σ standard deviation calculated for each cluster. The blue, grey and black lines show the linear regression between the average mass of *E. huxleyi* coccoliths and the considered environmental parameters for clusters #1, #2 and #3. The green dotted line shows the linear regression between the mass of *E. huxleyi* coccoliths and the considered environmental parameters for the entire data set (for the *r* values refer to Table 2).

2.3 Statistical methods

In order to identify the environmental parameters that govern the mass of *E. huxleyi* coccoliths in the surface-sediment samples, we first performed a hierarchical cluster analysis (HCA) on the standardized values of the environmental parameters in seawater (temperature and salinity; nitrate, phosphate and chlorophyll *a* concentrations; and pH, pCO_2, and $[CO_3^{2-}]$). This first step was necessary to highlight the areas (clusters) with characteristic physicochemical properties. We used the Ward method (Ward, 1963) and squared Euclidian distance in order to minimize the total within-cluster variance (Ward, 1963). The dendrogram is presented in the Supplement, Fig. S3 and the derived map of the main clusters shown in Fig. 3a. Then we performed principal component analyses (PCA) on the standardized values of the environmental parameters and the mass of *E. huxleyi*. In a first step, the PCA was conducted on the entire data set in order to have an overview, and in a second step we conducted the same analyses on the parameters of the different clusters. Figure S4 of the Supplement presents the results of the PCA, while Table 2 presents the correlation between the mass of

E. huxleyi and the environmental parameters. The correlation coefficients between each environmental parameter and the mass of *E. huxleyi* for the different clusters and the entire data set is provided in the Supplement (Table S1). All these analyses were performed using SPSS (Statistical Package for the Social Sciences; version 10.1) statistical software.

3 Results

3.1 Coccolith calcite mass and clustering

A total of 19 982 coccoliths belonging to the family Noëlaerhabdaceae were analyzed from surface sediment samples retrieved from the South Atlantic, the subantarctic, the Agulhas System, and the southwestern Indian oceans (Fig. 1). Among them 10 333 were *E. huxleyi* while the remaining 9649 were placoliths belonging to the genera *Gephyrocapsa* and *Reticulofenestra*. Although results discussed below focus exclusively on *E. huxleyi*, we also measured the average mass of all the specimens belonging to the family Noëlaerhabdaceae (presented in the discussion) in order to compare our results with those of a recent study that uses a similar approach from other oceanic regions (Beaufort et al., 2011). For each coccolith, the length (in µm) and the mass of calcite (in pg) were measured. The calcite mass of *E. huxleyi* coccolith is on average 3.12 pg ($n = 10\,333$, $\sigma = 0.66$), with values ranging between 1.73 pg ($n = 101$, $\sigma = 0.69$) in sample ANT2606-3 (53°22′ S, 41°21′ E, 2552 m water depth) and 4.85 pg ($n = 209$, $\sigma = 2.23$) in sample ANT2561-1 (42°26′ S, 28°57′ E, 4471 m water depth) (Figs. 1, 3b–i). For coccoliths belonging to Noëlaerhabdaceae (also including *E. huxleyi*), the averaged mass of calcite is 10.17 pg ($\sigma = 9.92$).

The results of the HCA performed on the environmental parameters show that the 70 samples can be divided into 3 clusters (Figs. 3a, S3): cluster #1 encompasses a total of 33 samples distributed along the Agulhas System, between the subtropical front and the South Atlantic Gyre, and north to the Atlantic Gyre (Fig. 3a). These samples are characterized by the highest range of values for Chl *a* (0.07–0.43 mg m^{-3}), pH (8.07–8.23) and pCO_2 (231.51–354.51 µatm) (Fig. 3d, g, h), and the lowest range of values for $[CO_3^{2-}]$ (222.54–260.21 µmol kg^{-1}) (Fig. 3i). Cluster #2 encompasses a total of 19 samples, all situated within the South Atlantic Gyre (Fig. 3a) with the smallest range of values in temperature (22.64–24.42 °C), salinity (36.42–36.92 psu), Chl *a* (0.04–0.08 mg m^{-3}), nitrate (0.1–1.39 mmol m^{-3}) and phosphate (0.16–0.23 mmol m^{-3}) (Fig. 3b–f). The very low variability of nutrient concentrations within cluster #2 reflects the oligotrophic conditions that prevail in the South Atlantic Gyre (Morel et al., 2010). Finally, cluster #3 includes the remaining 18 samples all situated south of the subtropical front (Fig. 3a). This cluster corresponds to a region with the largest physicochemical gradients in temperature (from 1.80–16.45 °C), salinity (33.86–35.25 psu), nitrate (2.69–25.18 mmol m^{-3}), phosphate (0.47–1.77 mmol/m^3), and $[CO_3^{2-}]$ (131.32–240.70 µmol kg^{-1}) (Fig. 3b, c, e, f, i), but not pH (8.205–8.286) and pCO_2 (203.03–251.83 µatm) (Fig. 3g, h).

When we compare the averaged mass of *E. huxleyi* within the different clusters, it appears that the mass is highest within cluster #3 (3.6 ± 0.82 pg) followed by cluster #1 (3.1 ± 0.48 pg) and cluster #2 (2.7 ± 0.49 pg). Further, a similar pattern is observed when considering the whole range of values covered by the mass of *E. huxleyi* within the three clusters (Fig. 3b–i): cluster #3 presents the highest range of values (1.73–4.85 pg), since the two samples with the lowest and highest *E. huxleyi* mass belong to this cluster, followed by cluster #1 (2.02 pg) and cluster #2 (1.7 pg).

3.2 PCA

Results of the PCA conducted on the entire data set show that ∼ 80 % of the variance can be explained by two factors (see Supplement, Fig. S4a). The first factor (F1), which explains ∼ 60 % of the variance, is driven (in order of importance) by temperature (18 % of F1), phosphate (16.3 %), nitrate (15.6 %), salinity (15.3 %), $[CO_3^{2-}]$ (14.7 %), and the mass of *E. huxleyi* (2.7 %). The second factor (F2) explains 20 % of the variance within the samples and is driven by the pCO_2 (33.6 % of F2), the pH (32.9 %) and the Chl *a* (16.4 %), the other parameters having very low scores. Interestingly, these results show that the mass of *E. huxleyi* presents a significant correlation (at the 95 % confidence level) with all the parameters, except nitrate and phosphate (Table 2): the most important being, according to the *r* values, Chl *a*, pCO_2, salinity, pH, temperature, and $[CO_3^{2-}]$.

Results of the PCA conducted on the samples of cluster #1 (Agulhas System and South Atlantic Gyre edges) show that ∼ 73.5 % of the variance within the samples can be explained by 2 factors (see Fig. S4b). The first factor (F1), which explains ∼ 43 % of the variance, is driven (in order of importance) by temperature (22.9 % of F1), pH (20 %), pCO_2 (19.5 %), salinity (12.8 %) and the mass of *E. huxleyi* (8.5 %). The second factor (F2) explains ∼ 30.4 % of the variance within the samples and is driven by nitrate (25 % of F2), phosphate (19.6 %), Chl *a* (18.8 %), and $[CO_3^{2-}]$ (14.9 %). These analyses show that the mass of *E. huxleyi* presents a significant correlation (within a 95 % confidence interval) with pH, pCO_2, and temperature (Table 2). This suggests a possible influence of both carbonate system parameters (i.e., $[CO_3^{2-}]$) and temperature on the calcite mass of *E. huxleyi*.

Results of the PCA conducted on the samples of cluster #2 (South Atlantic Gyre) show that ∼ 75.6 % of the variance within the samples can be explained by two factors (see Supplement, Fig. S4c). The first factor (F1), which explains ∼ 48 % of the variance, is driven (in order of importance) by nitrate (17.2 % of F1), phosphate (16.9 %), Chl *a* (16.2 %), the mass of *E. huxleyi* (14.5 %) and $[CO_3^{2-}]$ (10.5 %). The second factor (F2) explains ∼ 27.7 % of the variance within

Table 2. Coefficients of correlation between the mass of *E. huxleyi* and the environmental parameters for the three clusters and the entire data set. The values in bold are significant ($p < 0.0001$).

	Temperature	Salinity	Chl *a*	Nitrate	Phosphate	pH	pCO_2	$[CO_3^{2-}]$
Cluster #1	**−0.537**	−0.225	−0.155	−0.116	0.022	**0.621**	**−0.605**	0.018
Cluster #2	0.252	0.197	**−0.652**	**−0.660**	**−0.704**	0.383	−0.391	0.371
Cluster #3	**0.609**	**0.562**	**0.557**	**−0.632**	**−0.620**	−0.163	0.090	**0.554**
Entire data set	**−0.305**	**−0.359**	**0.406**	0.088	0.134	**0.356**	**−0.372**	**−0.268**

the samples and is driven by the pCO_2 (21.8 % of F2), pH (21.7 %), temperature (19.9 %) and salinity (16.8 %). These analyses show that the mass of *E. huxleyi* presents a significant correlation (within a 95 % confidence interval) with phosphate, nitrate, and Chl *a* (Table 2), highlighting a possible nutrient influence on the calcite mass of *E. huxleyi*.

Finally, the results of the PCA conducted on the samples of the cluster #3 (Southern Ocean) show that ∼ 90 % of the variance within the samples can be explained by two factors (see Fig. S4d). The first factor (F1), which explains ∼ 68.2 % of the variance, is driven (in order of importance) by temperature (16 % of F1), nitrate (15.8%), phosphate (15.7 %), salinity (15.5 %), $[CO_3^{2-}]$ (15.3 %), Chl *a* (14 %) and the mass of *E. huxleyi* (7.4 %). The second factor (F2) explains ∼ 22.5 % of the variance within the samples and is driven by pCO_2 (49.1 % of F2) and pH (48.4 % of F2). These analyses show that the mass of *E. huxleyi* presents a significant correlation (within a 95 % confidence interval) with all the parameters except pH and pCO_2 (Table 2), the most important being nitrate, phosphate, temperature, salinity, Chl *a*, and $[CO_3^{2-}]$. This suggests a possible influence of the surface hydrography, the nutrients and to a lesser degree the $[CO_3^{2-}]$ on the calcite mass of *E. huxleyi*.

4 Discussion

We investigated the variations of *E. huxleyi* calcite mass in sediment samples deposited under late-Holocene to pre-anthropogenic conditions in the South Atlantic, Southern Ocean, Agulhas System, and southwestern Indian Ocean, and compared them with environmental parameters (temperature, salinity, nutrients and carbonate chemistry). According to the HCA, the entire data set can be divided into three regional clusters (Fig. 3a). The PCA performed on the samples of the Agulhas system and the South Atlantic Gyre edges (cluster #1) show high correlation between the calcite mass of *E. huxleyi* and temperature, pCO_2 and pH; whereby low calcite mass is associated to high temperature, high pCO_2 and low pH (Table 2). This area is characterized by the highest variability in surface productivity (Chl *a*), pCO_2, and pH (Fig. 3d, g, h). Previous studies show that temperature can influence *E. huxleyi* coccolith mass or size: more heavily calcified specimens were observed in regions where sea surface temperature was the highest (Beaufort and Heussner, 2001; Beaufort et al., 2008). However, our results tend to show the opposite within cluster #1 (Table 2). Moreover, the correlation between the mass and these parameters within the two others clusters is different: it is positive in cluster #3 and not significant within cluster #2 (Table 2). It is then hard to decipher if and how temperature could influence the mass of *E. huxleyi*. However, it has been shown that elevated pCO_2 can have a negative impact on the coccolith morphogenesis in culture experiments (de Bodt et al., 2010; Bach et al., 2012), which is in agreement with our findings (Table 2).

The South Atlantic Gyre (cluster #2) presents the lowest variability in temperature, salinity, Chl *a*, and nutrient concentrations of the entire data set (Fig. 3b–f). The results of the PCA show that *E. huxleyi* calcite mass is exclusively (negatively) correlated to the surface productivity and the nutrient concentrations (Table 2). The oligotrophy characterizing the South Atlantic Gyre (Morel et al., 2010) (Fig. 3e, f) could lead to an increase of *E. huxleyi* calcite mass. Indeed, such impact of nutrient limitation on *E. huxleyi* calcite mass has already been observed (Paasche, 1998; Müller et al., 2008; Oviedo et al., 2014), and it is likely related to the impact of nutrient limitation on different phases of the cell cycle during mitosis (Müller et al., 2008). In this particular case, *E. huxleyi* appears to be very sensitive to small variations in nutrient concentrations.

Finally, the samples of the Southern Ocean (cluster #3) are characterized by the highest range in values for temperature, salinity, nutrient concentrations and $[CO_3^{2-}]$ (Fig. 3b, c, e, f, i) of the entire data set. Within this cluster, *E. huxleyi* calcite mass shows high correlations with all these parameters (Table 2); an increase of temperature, salinity, Chl *a*, $[CO_3^{2-}]$ and a decrease of nitrate and phosphate are concomitant to an increase of *E. huxleyi* calcite mass. Such impact of temperature (Beaufort and Heussner, 2001; Beaufort et al., 2008), salinity (Bollmann and Herrle, 2007; Bollmann et al., 2009), nutrient concentrations (Paasche, 1998; Müller et al., 2008; Oviedo et al., in review) and $[CO_3^{2-}]$ on the averaged calcite mass of *E. huxleyi* has been previously documented.

If the entire data set is considered, most of the environmental parameters (temperature, salinity and carbonate chemistry) present a significant correlation with *E. huxleyi* calcite mass (Table 2), suggesting the importance of synergistic effects of the environmental factors. Although the environmental parameters are often correlated with each other, leading

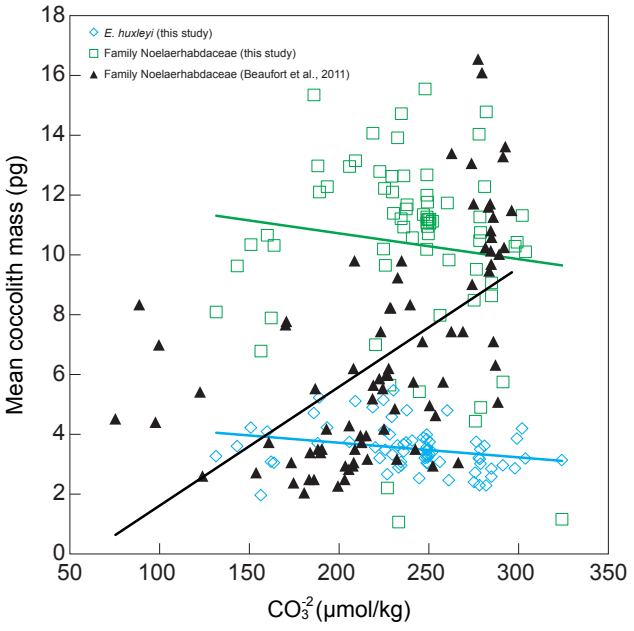

Fig. 4. Comparison between the averaged mass of *E. huxleyi* (this study, open blue diamonds), the averaged mass of the coccoliths belonging to the family Noëlaerhabdaceae in the surface sediment (including *E. huxleyi*, this study, green open squares), the averaged mass of the coccoliths belonging to the family Noëlaerhabdaceae in the plankton (including *E. huxleyi*, Beaufort et al., 2011, black triangles) and the carbonate ion concentration ($[CO_3^{2-}]$). The blue, green and black lines show the linear regression for the three data sets.

to a multiple correlations (Table 2 and Table S1 of the Supplement), we interpret this evidence as indicative of a combined influence of productivity, carbonate system, and the surface ocean hydrography on the mass of *E. huxleyi*. However, follow-up studies, involving culture experiments and in situ measurements (e.g., Henderiks et al., 2012; Charampopolou et al., 2011; Poulton et al., 2013), are needed to better constrain the synergistic effects of these environmental parameters on *E. huxleyi* calcite mass variations.

We cannot rule out the possibility that the variability of the calcite mass that we observed reflects the regional distribution in *E. huxleyi* morphotypes (Boeckel and Baumann, 2008; Smith et al., 2013). In our study, *E. huxleyi* morphotypes are not differentiated since they cannot be identified when using a light microscope; this is as true for the human eye as for SYRACO. However, previous results based on SEM investigation of surface sediment samples along a N–S transect from the South Atlantic Subtropical Gyre to the subantarctic zone show that the most soluble resistant *E. huxleyi* morphotype (type A) (Boeckel and Baumann, 2008) largely dominates the morphotype composition.

Current knowledge of the factors that control the coccolith mass variability suggests a prominent role of the seawater carbonate system (e.g., Riebesell et al., 2000; Beaufort et al., 2011; Riebesell and Tortell, 2011 and references therein). A reduction of ∼ 25 % coccolith mass has been linked to an increase by 100 ppmv of the atmospheric CO_2 (Beaufort et al., 2011); that is, the amplitude of the change in atmospheric CO_2 concentrations seen across the late-Pleistocene glacial–interglacial transitions (Mönnin et al., 2001; Lüthi et al., 2008). *Emiliania huxleyi* is present with numerous ecotypes that likely justify its dominance in the coccolith assemblages over the last ∼ 80 000 yr (Thierstein et al., 1977; Read et al., 2013). The calcification of its coccoliths appears strongly biologically regulated and genetic analyses may likely provide further insights into the mechanisms controlling the coccolith mass in different *E. huxleyi* strains (Paasche, 2001). An open issue is to understand the combined environmental conditions that can prompt different feedbacks during calcification (e.g., Müller et al., 2012). The seawater carbonate chemistry impact on coccolith mass has been mainly studied in experimental culture settings and secondarily with in situ observations. These studies highlight the uneven responses of coccolith calcification (Ridgwell et al., 2009). The environmental conditions of seawater induce changes in coccolithophore cell division rate and calcification, and in the particulate organic and inorganic carbon production (Müller et al., 2008). The seawater carbonate system, and in particular $[CO_3^{2-}]$, is an important regulator of coccolithophore calcification and the understanding of its role in this process is currently a subject of intense debate (Bach et al., 2011 and references therein). We compare here the data compilation of Beaufort et al. (2011) based on living coccolithophore water samples to the present study (Fig. 4). Since the authors compare the mass of coccolith belonging to the family Noëlaerhabdaceae (including the genera *Emiliania*, *Gephyrocapsa*, and *Reticulofenestra*) to $[CO_3^{2-}]$, we provide the estimation of the averaged mass of the coccoliths belonging to the family Noëlaerhabdaceae (Fig. 4). Despite the fact that the two data sets (Beaufort et al., 2011 and this study) present a very similar range of coccolith calcite mass, no significant correlation between $[CO_3^{2-}]$ and the calcite mass of the family Noëlaerhabdaceae is found in our data set (Fig. 4). Indeed, water samples reproduce local and seasonal oceanographic conditions of living specimens, a "snapshot" in time. However, sediment samples are a multidecadal-weighted average of the physicochemical influence of overlying water masses on the calcification of *E. huxleyi* (Ziveri et al., 2000; Broerse et al., 2000), and a recent comparison of plankton and surface sediments by Boeckel and Baumann (2008) revealed that the distribution of the morphotypes is reflected in the sedimentary archive.

Our study provides statistical evidence for a relationship between *E. huxleyi* calcification and physicochemical properties of seawater under preindustrial conditions, i.e., when the carbonate chemistry forcing on the calcifying organisms was plausibly much weaker than today (Feely et al., 2004). The results emphasize the potential role of nutrients (phosphate and nitrate) and carbonate chemistry (pH and pCO_2)

in determining *E. huxleyi* coccolith mass, in line with other studies on foraminifera (Aldridge et al., 2012; Bijma et al., 2002; Barker and Elderfield, 2002). The combined influence of different factors on calcification seems to be a more robust assumption than a sole abiotic parameter influencing marine calcification in the preindustrial time.

5 Conclusions

There is currently much debate on the response of calcifying planktonic organisms (e.g., coccolithophores, foraminifera, pteropods) to the ongoing seawater acidification (Doney et al., 2009; Kroeker et al., 2013). By examining a suite of 70 surface sediment samples from the South Atlantic, the Agulhas System, and the Southern Ocean we found that it is the combined effect of nutrients and seawater carbonate chemistry controlling coccolithophore mass in preanthropogenic conditions. There is a regional difference in terms of dominant controlling environmental parameters on coccolith mass. For example in the Agulhas Current and the samples surrounding the South Atlantic Gyre the main factor is carbonate chemistry (largest range in pCO_2 and pH) and for the South Atlantic Gyre nutrients (oligotrophy) are key. Further south is characterized by large physicochemical gradients, and the combined effects of seawater CO_3^{2-} and nutrients governing coccolith mass.

Although it is clear that these environmental gradients can have a profound impact on coccolithophore calcification, the combined effects of these abiotic factors makes singular cause–effect relations difficult to be conclusively determined. The ongoing human-influenced climatic and environmental changes, such as global warming, increased stratification, and ocean acidification (Gruber, 2011) have important consequences for calcification processes. Because of the ongoing rapid physicochemical alterations of the ocean, the evidence we report of multiple environmental factors affecting coccolithophore calcification provides important information for projecting the response of (bio)calcification in the near future. Finally, our results suggests that paleostudies on coccolith calcite mass should consider the possible effects of multiple environmental parameters when deciphering the response of coccolithophore calcification to past atmospheric CO_2 fluctuations.

Supplementary material related to this article is available online at http://www.biogeosciences.net/11/2295/2014/bg-11-2295-2014-supplement.zip.

Acknowledgements. We are indebted to I. R. Hall and R. Zahn for the surface sediment samples from the Agulhas region. M. T. Horigome was supported by a studentship of the Joint European Master in Environmental Studies Consortium. P. Ziveri, M. Grelaud, G. Marino, and P. G. Mortyn thank the Spanish Ministry of Science and Innovation for funding this study (PROCARSO, grant no. CGL2009-10806; CTM2008-04365-E). G. Marino acknowledges support from the Universitat Autonoma de Barcelona (postdoctoral research grant PS-688-01/08). Suggestions and constructive criticisms by J. Henderiks, M. Bordiga, A. Poulton, C. Daniels, J. Hopkins, S. O'Dea, N. Percival, R. Sheward, H. Smith, one anonymous reviewer and by the BG associate editor Christine Klaas greatly improved the manuscript. This work contributes to the EU FP7 project: Mediterranean Sea Acidification under a changing climate (grant agreement no. 265103).

Edited by: C. Klaas

References

Aldridge, D., Beer, C. J., and Purdie, D. A.: Calcification in the planktonic foraminifera *Globigerina bulloides* linked to phosphate concentrations in surface waters of the North Atlantic Ocean, Biogeosciences, 9, 1725–1739, doi:10.5194/bg-9-1725-2012, 2012.

Bach, L. T., Riebesell, U., and Schulz, K. G.: Distinguishing between the effects of ocean acidification and ocean carbonation in the coccolithophore *Emiliania huxleyi*, Limnol. Oceanogr., 56, 2040–2050, doi:10.4319/lo.2011.56.6.2040, 2011.

Bach, L. T., Bauke, C., Meier, K. J. S., Riebesell, U., and Schulz, K. G.: Influence of changing carbonate chemistry on morphology and weight of coccoliths formed by *Emiliania huxleyi*, Biogeosciences, 9, 3449–3463, doi:10.5194/bg-9-3449-2012, 2012.

Baith, K., Lindsay, R., Fu, G., and McClain, C. R.: Data analysis system developed for ocean color satellite sensors, EOS Transactions AGU, 82, 202–202. doi:10.1029/01eo00109, available at: http://oceancolor.gsfc.nasa.gov/seadas/, 2001.

Banse, K.: Low seasonality of low concentrations of surface chlorophyll in the Subantarctic water ring: underwater irradiance, iron, or grazing?, Prog. Oceanogr., 37, 241–291, doi:10.1016/S0079-6611(96)00006-7, 1996.

Barcelos e Ramos, J., Müller, M. N., and Riebesell, U.: Short-term response of the coccolithophore *Emiliania huxleyi* to an abrupt change in seawater carbon dioxide concentrations, Biogeosciences, 7, 177–186, doi:10.5194/bg-7-177-2010, 2010.

Barker, S. and Elderfield, H.: Foraminiferal calcification response to glacial-interglacial changes in atmospheric CO_2, Science, 297, 833–836, 2002.

Baumann, K.-H., Boeckel, B., Donner, B., Gerhardt, S., Henrich, R., Vink, A., Volbers, A., Willems, H., and Zonneveld, K. A. F.: Contribution of calcareous plankton groups to the carbonate budget of South Atlantic surface sediments, in: The South Atlantic in the Late Quaternary; Reconstruction of Material Budget and Current Systems, edited by: Wefer, G., Mulitza, S., and Ratmeyer, V., Springer-Verlag, Berlin, 81–99, 2004.

Båtvik, H., Heimdal, B. R., Fagerbakke, K. M., and Green, J. C.: Effects of unbalanced nutrient regime on coccolith morphology and size in *Emiliania huxleyi* (Prymnesiophyeae), Eur. J. Phycol., 32, 155–165, 1997.

Beaufort, L. and Heussner, S.: Coccolithophorids on the continental slope of the Bay of Biscay: production, transport and contribution to mass fluxes, Deep Sea Res. Pt II, 46, 2147–2174, 1999.

Beaufort, L. and Heussner, S.: Seasonal dynamics of calcareous nannoplankton on a West European continental margin: the Bay of Biscay, Mar. Micropaleont., 43, 27–55, 2001.

Beaufort, L. and Dollfus, D.: Automatic recognition of coccolith by dynamical neural network, Mar. Micropaleont., 51, 57–73, 2004.

Beaufort, L.: Weight estimates of coccoliths using the optical properties (birefringence) of calcite, Micropaleont., 51, 289–298, 2005.

Beaufort, L., Couapel, M., Buchet, N., Claustre, H., and Goyet, C.: Calcite production by coccolithophores in the south east Pacific Ocean, Biogeosciences, 5, 1101–1117, doi:10.5194/bg-5-1101-2008, 2008.

Beaufort, L., Probert, I., de Garidel-Thoron, T., Bendif, E. M., Ruiz-Pino, D., Metzl, N., Goyet, C., Buchet, N., Coupel, P., Grelaud, M., Rost, B., Rickaby, R. E. M., and de Vargas, C.: Sensitivity of coccolithophores to carbonate chemistry and ocean acidification, Nature, 476, 80–83, 2011.

Berger, W. H.: Biogenous deep-sea sediments: production, preservation and interpretation, in: Chemical Oceanography, edited by: Riley, J. P., and Chester, R., Academic Press, London, New York, 5, 265–389, 1976.

Bijma, J., Spero, H. J., and Lea, D. W.: Reassessing foraminiferal stable isotope geochemistery: Impact of the oceanic carbonate system (experimental results), in: Uses of Proxies in Paleoceanography: Examples from the South Atlantic, edited by: Fischer, G. and Wefer, G., Springer Verlag, Berlin-Heidelberg, 489–512, 1999.

Boeckel, B., Baumann, K.-H., Henrich, R., and Kinkel, R.: Coccolith distribution patterns in South Atlantic and Southern Ocean surface sediments in relation to environmental gradients, Deep-Sea Res. Pt. I, 53, 1073–1099, 2006.

Boeckel, B. and Baumann, K.-H.: Vertical and lateral variations in coccolithophore community structure across the subtropical frontal zone in the South Atlantic Ocean, Mar. Micropaleontol., 67, 255–373, doi:10.1016/j.marmicro.2008.01.014, 2008.

Bollmann, J., Henderiks, J., and Brabec, B.: Calibration of *Gephyrocapsa* coccolith abundance in Holocene sediments for paleotemperature assessment, Paleoceanography, 17, 1035, doi:10.1029/2001PA000742, 2002.

Bollmann, J. and Herrle, J. O.: Morphological variation of *Emiliania huxleyi* and sea surface salinity, Earth Planet. Sci. Lett., 255, 273–288, 2007.

Bollmann, J., Herrle, J. O., Cortés, M. Y., and Fielding, S. R.: The effect of sea water salinity on the morphology of *Emiliania huxleyi* in plankton and sediment samples, Earth Planet. Sci. Lett., 284, 320–328, doi:10.1016/j.epsl.2009.05.003, 2009.

Broerse, A. T. C., Ziveri, P., van Hinte, J. E., and Honjo, S: Export production, species composition, and coccolith-$CaCO_3$ fluxes in the NE Atlantic (34° N 21° W and 48° N 21° W), Deep Sea Res. Pt. II, 47, 1877–1905, 2000.

Bown P. R. and Young J. R.: Techniques, in: Calacareous Nannofossil Biostratigraphy, edited by: Bown, P. R., Chapman & Hall, London, 16–28, 1998.

Charalampopoulou, A., Poulton, A. J., Tyrrell, T., and Lucas, M. I.: Irradiance and pH affect coccolithophore community composition on a transect between the North Sea and the Arctic Ocean, Mar. Ecol. Prog. Ser., 431, 25–43, doi:10.3354/meps09140, 2011.

Delille, B., Harlay, J., Zondervan, I., Jacquet, S., Chou, L., Wollast, R., Bellerby, R. G. J., Frankignoulle, M., Borges, A. V., Riebesell, U., and Gattus, J. P.: Response of primary production and calcification to changes of pCO_2 during experimental blooms of the coccolithophorid *Emiliania huxleyi*, Global Biogeochem. Cy., 19, GB2023, doi:10.1029/2004GB002318, 2005.

de Bodt, C., Van Oostende, N., Harlay, J., Sabbe, K., and Chou, L.: Individual and interacting effects of pCO_2 and temperature on *Emiliania huxleyi* calcification: study of the calcite production, the coccolith morphology and the coccosphere size, Biogeosciences, 7, 1401–1412, doi:10.5194/bg-7-1401-2010, 2010.

Dollfus, D. and Beaufort, L.: Fat neural network for recognition of position-normalised objects, Neural Networks, 12, 553–560, 1999.

Doney, S. C., Fabry, V. J., Feely, R. A., and Kleypas, J. A.: Ocean acidification: the other CO_2 problem, Annu. Rev. Mar. Sci., 1, 169–192, 2009.

Fabry, V., Seibel, B. S., Feely, R. A., and Orr, J. C.: Impacts of ocean acidification on marine fauna and ecosystem processes, ICES J. Mar. Science, 65, 414–432, 2008.

Feely, R. A., Sabine, C. L., Lee, K., Berelson, W., Kleypas, J., Fabry, V. J., and Millero, F. J.: Impact of anthropogenic CO_2 on the $CaCO_3$ system in the oceans, Science, 305, 362–366, 2004.

Feldman, G. C. and McClain, C. R.: Ocean Color Web, MODIS Reprocessing L3, NASA Goddard Space Flight Center, edited by: Kuring, N., Bailey, S. W., available at: http://oceancolor.gsfc.nasa.gov/, 2011.

Fielding, S. R., Herrle, J. O., Bollmann, J., Worden, R. H., and Montagnes, D. J. S.: Assessing the applicability of *Emiliania huxleyi* coccolith morphology as a sea-surface salinity proxy, Limnol. Oceanogr., 54, 1475–1480, 2009.

Fischer, G. and Karakaş, G.: Sinking rates and ballast composition of particles in the Atlantic Ocean: implications for the organic carbon fluxes to the deep ocean, Biogeosciences, 6, 85–102, doi:10.5194/bg-6-85-2009, 2009.

Foster, G. L.: Seawater pH, pCO_2 and $[CO_3^{2-}]$ variations in the Caribbean Sea over the last 130 kyr: A boron isotope and B/Ca study of planktic foraminifera, Earth Planet. Sci. Lett., 271, 254–266, doi:10.1016/j.epsl.2008.04.015, 2008.

Frenz, M., Baumann, K.-H., Boeckel, B., Höppner, R., and Herich, R.: Quantification of foraminifer and coccolith carbonate in south atlantic surface sediments by means of carbonate grain-size distributions, J. Sediment. Res., 75, 464–475, 2005.

Gouretski, V. V. and Koltermann, K. P.: WOCE global hydrographic climatology, available at: http://odv.awi.de/en/data/ocean/woce_global_hydrographic_climatology/, 2004.

Goyet, C., Healy, R., and Ryan, J.: Estimated alkalinity and total dissolved inorganic carbon, available at: http://odv.awi.de/en/data/ocean/global_alkanity_tco2/, 2000.

Gruber, N.: Warming up, turning sour, losing breath: ocean biogeochemistry under global change, Philosophical Transactions of the

Royal Society A: Mathematical, Phys. Engineer. Sci., 369, 1980–1996, doi:10.1098/rsta.2011.0003, 2011.

Hagino, K., Okada, H., and Matsuoka, H.: Coccolithophore assemblages and morphotypes of *Emiliania huxleyi* in the boundary zone between the cold Oyashio and warm Kuroshio currents off the coast of Japan, Mar. Micropaleont., 55, 19–47, 2005.

Henderiks, J., Winter, A., Elbrächter, M., Feistel, R., van der Plas, A., Nausch, G., and Barlow, R.: Environmental controls on *Emiliania huxleyi* morphotypes in the Benguela coastal upwelling system (SE Atlantic), Mar. Ecol.-Prog. Ser., 448, 51–66, doi:10.3354/meps09535, 2012.

Hönisch, B. and Hemming, N. G.: Surface ocean pH response to variations in pCO_2 through two full glacial cycles, Earth Planet Sci. Lett., 236, 305-314, doi:10.1016/j.epsl.2005.04.027, 2005.

Honjo, S.: Dissolution of suspended coccoliths in the deep-sea water column and sedimentation of coccolith ooze, in: Dissolution of Deep-Sea Carbonates, edited by: Sliter, W. V., Bé, A. W. H., and Berger, W.H., Volume Special Publication 13, Cushman Foundation Foraminiferal Research, 114–128, 1975.

Iglesias-Rodriguez, M. D., Halloran, P. R., Rickaby, R. E. M., Hall, I. R., Colmenero-Hidalgo, E., Gittins, J. R., Green, D. R. H., Tyrrell, T., Gibbs, S. J., von Dassow, P., Rehm, E., Armbrust, E. V., and Boessenkool, K. P.: Phytoplankton calcification in a high-CO_2 world, Science, 320, 336–340, doi:10.1126/science.1154122, 2008.

Jonkers, L., de Nooijer, L. J., Reichart, G.-J., Zahn, R., and Brummer, G.-J. A.: Encrustation and trace element composition of *Neogloboquadrina dutertrei* assessed from single chamber analyses – implications for paleotemperature estimates, Biogeosciences, 9, 4851–4860, doi:10.5194/bg-9-4851-2012, 2012.

Kroeker, K. J., R. L. Kordas, R. Crim, I. E. Hendriks, L. Ramajo, G. S. Singh, C. M. Duarte, and Gattuso, J.-P.: Impacts of ocean acidification on marine organisms: quantifying sensitivities and interaction with warming, Glob. Change Biol., 19, 1884–1896, doi:10.1111/gcb.12179, 2013.

Langer, G., Geisen, M., Baumann, K.-H., Kläs, J., Riebesell, U., Thoms, S., and Young, J. R.: Species-specific responses of calcifying algae to changing seawater carbonate chemistry, Geochem. Geophy. Geosy., 7, Q09006, doi:10.1029/2005GC001227, 2006.

Langer, G., Nehrke, G., Probert, I., Ly, J., and Ziveri, P.: Strain-specific responses of *Emiliania huxleyi* to changing seawater carbonate chemistry, Biogeosciences, 6, 2637–2646, doi:10.5194/bg-6-2637-2009, 2009.

Langer, G., Probert, I., Nehrke, G., and Ziveri, P.: The morphological response of *Emiliania huxleyi* to seawater carbonate chemistry changes: an inter-strain comparison, J. Nannoplankton Res., 32, 29–34, 2011.

Lewis, E. and Wallace, D. W. R.: Program Developed for CO_2 System Calculations, ORNL/CDIAC-105, Carbon Dioxide Information Analysis Center, Oak Ridge National Laboratory, US Department of Energy, 1998.

Lohbeck, K. T., Riebesell, U., and Reusch, T. B. H.: Adaptive evolution of a key phytoplankton species to ocean acidification, Nat. Geosci., 5, 917–917, doi:10.1038/ngeo1637, 2012.

Lüthi, D., Le Floch, M., Bereiter, B., Blunier, T., Barnola, J.-M., Siegenthaler, U., Raynaud, D., Jouzel, J., Fischer, H., Kawamura, K., and Stocker, T. F.: High-resolution carbon dioxide concentration record 650,000–800,000 years before present, Nature, 453, 379–382, 2008.

Lutjeharms, J. R. E.: The Agulhas Current, Springer, 330 pp., 2006.

Martínez-Méndez, G., R. Zahn, I. R. Hall, F. J. C. Peeters, L. D. Pena, I. Cacho, and Negre, C.: Contrasting multiproxy reconstructions of surface ocean hydrography in the Agulhas Corridor and implications for the Agulhas Leakage during the last 345,000 years, Paleoceanography, 25, PA4227, doi:10.1029/2009pa001879, 2010.

Mizuki, T., Lynne, D. T., and Michael, S. M.: Water-mass distributions in the western South Atlantic; a section from South Georgia Island (54S) northward across the equator, J. Mar. Res., 52, 55–81, doi:10.1357/0022240943076759, 1994.

Mollenhauer, G.: Organic Carbon accumulation in the South Atlantic: Sedimentary processes and Glacial/Interglacial budgets. Berichte FB Geowissenschaften, Univ. Bremen, 204, 1–139, 2002.

Mollenhauer, G., Eglinton, T. I., Ohkouchi, N., Schneider, R. R., Müller, P. J., Grootes, P. M., and Rullkötter, J.: Asynchronous alkenone and foraminifera records from the Benguela Upwelling System, Geochim. Cosmochim. Acta, 67, 2157–2171, 2003.

Mollenhauer, G., Schneider, R. R., Jennerjahn, T. C., Müller, P. J., and Wefer, G.: Organic carbon accumulation in the South Atlantic Ocean: its modern, mid-Holocene and last glacial distribution, Global Planet. Change, 40, 249–266, doi:10.1016/j.gloplacha.2003.08.002, 2004.

Mollenhauer, G., Inthorn, M., Vogt, T., Zabel, M., Sinninghe Damsté, J. S., and Eglinton, T. I.: Aging of marine organic matter during cross-shelf lateral transport in the Benguela upwelling system revealed by compound-specific radiocarbon dating, Geochem. Geophys. Geosys., G3, 8, Q09004, doi:10.1029/2007GC001603, 2007.

Mönnin, E., Indermühle, A., Dällenbach, A., Flückiger, J., Stauffer, B., Stocker, T. F., Raynaud, D., and Barnola, J.-M.: Atmospheric CO_2 concentrations over the last glacial termination, Science, 291, 112–114, 2001.

Morel, A., Claustre, H., and Gentili, B.: The most oligotrophic subtropical zones of the global ocean: similarities and differences in terms of chlorophyll and yellow substance, Biogeosciences, 7, 3139–3151, doi:10.5194/bg-7-3139-2010, 2010.

Müller, M. N., Antia, A. N., and LaRoche, J.: Influence of cell cycle phase on calcification in the coccolithophore *Emiliania huxleyi*, Limnol. Oceanogr., 53, 506–512, 2008.

Müller, M. N., Schulz, K. G., and Riebesell, U.: Effects of long-term high CO_2 exposure on two species of coccolithophores, Biogeosciences, 7, 1109–1116, doi:10.5194/bg-7-1109-2010, 2010.

Müller, M. N., Beaufort, L., Bernard, O., Pedrotti, M. L., Talec, A., and Sciandra, A.: Influence of CO_2 and nitrogen limitation on the coccolith volume of *Emiliania huxleyi* (Haptophyta), Biogeosciences, 9, 4155–4167, doi:10.5194/bg-9-4155-2012, 2012.

Okada, H. and Honjo, S.: The distribution of oceanic coccolithophorids in the Pacific, Deep-Sea Res. Pt. I, 20, 355–374, 1973.

Okada, H. and McIntyre, A.: Modern coccolithophores of the Pacific and North Atlantic oceans, Micropaleontology, 23, 1–54, 1977.

Orsi, A. H., Whitworth III, T., and Nowlin, W.: On the meridional extent and fronts of the Antarctic Circumpolar Current, Deep-Sea Res., 42, 641–673, 1995.

Oviedo, A., Langer, G., and Ziveri, P.: Effect of phosphorus limitation on calcification and element ratios in Mediterranean strains

of the coccolithophore *Emiliania huxleyi*, J. Exp. Mar. Biol. Ecol., in review, 2014.

Paasche, E.: Roles of nitrogen and phosphorus in coccolith formation in *Emiliania huxleyi* (Prymnesiophyceae), Eur. J. Phycol., 33, 33–42, 1998.

Paasche, E.: A review of the coccolithophorid *Emiliania huxleyi* (Prymnesiophyceae), with particular reference to growth, coccolith formation, and calcification-photosynthesis interactions, Phycologia, 40, 503–529, 2001.

Peterson, R. G. and Stramma, L.: Upper-level circulation in the South Atlantic Ocean, Prog. Oceanogr., 26, 1–73,1991.

Ploug, H., Iversen, M. H., Koski, M., and Buitenhuis, E. T.: Production, oxygen respiration rates, and sinking velocity of copepod fecal pellets: direct measurements of ballasting by opal and 25 calcite, Limnol. Oceanogr., 53, 469–476, 2008.

Popp, B. N., Kenig, F., Wakeham, S. G., Rust, T. M., Tilbrook, B., Griffiths, F. B., Wright, S. W., Marchant, H. J., Bidigare, R. R., and Laws, E. A.: Controls on the carbon isotopic composition of Southern Ocean phytoplankton, Global Biogeochem. Cy., 13, 827–843, 1999.

Poulton, A. J., Painter, S. C., Young, J. R., Bates, N. R., Bowler, B., Drapeau, D., Lyczsckowski, E., and Balch, W. M.: The 2008 *Emiliania huxleyi* bloom along the Patagonian Shelf: Ecology, biogeochemistry, and cellular calcification, Glob. Biogeochem. Cy., 2013GB004641, doi:10.1002/2013gb004641, 2013.

Raven, J., Caldeira, K., Elderfield, H., Hoegh-Guldberg, O., Liss, P., Riebesell, U., Shepherd, J., Turley, C., and Watson, A.: Acidification due to increasing carbon dioxide, Tech. Rep., The Royal Society, 2005.

Read, B. A., Kegel, J., Klute, M. J., Kuo, A., Lefebvre, S. C., Maumus, F., Mayer, C., Miller, J., Monier, A., Salamov, A., Young, J., Aguilar, M., Claverie, J.-M., Frickenhaus, S., Gonzalez, K., Herman, E. K., Lin, Y.-C., Napier, J., Ogata, H., Sarno, A. F., Shmutz, J., Schroeder, D., de Vargas, C., Verret, F., von Dassow, P., Valentin, K., Van de Peer, Y., Wheeler, G., Emiliania huxleyi Annotation Consortium, Dacks, J. B., Delwiche, C. F., Dyhrman, S. T., Glöckner, G., John, U., Richards, T., Worden, A. Z., Zhang, X., and Grigoriev, I. V.: Pan genome of the phytoplankton Emiliania underpins its global distribution, Nature, 499, 209–213, 2013.

Ridgwell, A. and Zeebe. R. E.: The role of the global carbonate cycle in the regulation and evolution of the Earth system, Earth Planet. Sci. Lett., 234, 299–315, 2005.

Ridgwell, A., Schmidt, D. N., Turley, C., Brownlee, C., Maldonado, M. T., Tortell, P., and Young, J. R.: From laboratory manipulations to Earth system models: scaling calcification impacts of ocean acidification, Biogeosciences, 6, 2611–2623, doi:10.5194/bg-6-2611-2009, 2009.

Riebesell, U., Zondervan, I., Rost, B., Tortell, P. D., Zeebe, R. E., and Morel, F. M. M.: Reduced calcification of marine plankton in response to increased atmospheric CO_2, Nature, 407,364–367, 2000.

Riebesell, U., Bellerby, R. G. J., Engel, A., Fabry, V. J., Hutchins, D. A., Reusch, T. B. H., Schulz, K. G., and Morel, F. M. M.: Comment on "Phytoplankton calcification in a high CO_2-world", Science, 322, 1466b, doi:10.1126/science.1161096, 2008.

Riebesell, U. and Tortell, P. D.: Effects of ocean acidification on pelagic organisms and ecosystems, in: Ocean Acidification, edited by: Gattuso, J.-P. and Hansson, L., Oxford University Press, Oxford, 99–121, 2011.

Rintoul, R. S.: Antarctic Circumpolar Current, Enc. Ocean Sci., 2nd Edn.,178–190, doi:10.1016/B978-012374473-9.00603-2, 2009.

Sabine, C. L., Feely, R. A., Gruber, N., Hey, R. M., Lee, K., Bullister, J. L., Wanninkhof, R., Wong, C. S., Wallace, D. W. R., Tilbrook, B., Millero, F. J., Peng, T.-H., Kozyr, A., Ono, T., and Rios, A. F.: The oceanic sink for anthropogenic CO_2, Science, 305, 367–371, doi:10.1126/science.1097403, 2004.

Schlitzer, R.: Ocean Data View, available at: http://odv.awi.de, 2009.

Sigman, D. M., Hain, M. P., and Haug, G. H.: The polar ocean and glacial cycles in atmospheric CO_2 concentration, Nature, 466, 47–55, doi:10.1038/nature09149, 2010.

Smith, H. E. K., Tyrrell, T., Charalampopoulou, A., Dumousseaud, C., Legge, O. J., Birchenough, S., Pettit, L. R., Garley, R., Hartman, S. E., Hartman, M. C., Sagoo, N., Daniels, C. J., Achterberg, E. P., and Hydes, D. J.: Predominance of heavily calcified coccolithophores at low $CaCO_3$ saturation during winter in the Bay of Biscay, Proc. Nat. Acad. Sci., 109, 8845–8849, doi:10.1073/pnas.1117508109, 2010.

Sokolov, S. and Rintoul, S. R.: Multiple jets of the Antarctic Circumpolar Current, J. Phys. Oceanogr., 37, 1394–1412, 2007.

Thierstein, H. R., Geitzenauer, K. R., Molfino, B., and Shackleton, N. J.: Global synchroneity of late Quaternary coccolith datum levels Validation by oxygen isotopes, Geology, 5, 400–404, doi:10.1130/0091-7613(1977)5<400:gsolqc>2.co;2, 1977.

Toggweiler, J. R., Russell, J. L., and Carson, S. R.: Mid latitude westerlies, atmospheric CO_2, and climate change during the ice ages, Paleoceanography, 21, PA2005, doi:10.1029/2005PA001154, 2006.

Van Cappellen, P.: Biomineralization and global biogeochemical cycles, in: Biomineralization, Mineralogical Reviews, vol. 54, edited by: Weiner, S., De Yoreo, J. J., and Dove, P., Mineralogical Society of America, 357–381, 2003.

Volbers, A. N. A. and Henrich, R.: Late Quaternary variations in calcium carbonate preservation of deep-sea sediments in the northern Cape Basin: results from a multiproxy approach, Mar. Geol., 180, 203–220, doi:10.1016/S0025-3227(01)00214-6, 2002.

Ward, J. H.: Hierarchical Grouping to Optimize an Objective Function, Journal of the American Statistical Association, 58, 236–244, doi:10.1080/01621459.1963.10500845, 1963.

Wefer, G., Mulitza, S., and Ratmeyer, V.: The South Atlantic in the Late Quaternary: Reconstruction of Material Budgets and Current Systems. Springer-Verlag Berlin Heidelberg New York, 2003.

Winter, A., Jordan, R. W., and Roth, P. H.: Biogeography of living coccolithophores in ocean waters, in: Coccolithophores, edited by: Winter, A. and Siesser, W. G., Cambridge University Press, Cambridge, 161–177, 1994.

Young, J. R. and Westbroek, P.: Genotypic variation in the coccolithophorid species *Emiliania huxleyi*, Mar. Micropaleontol., 18, 5–23, 1991.

Young J. R.: Functions of coccoliths, in: Coccolithophores, edited by: Winter, A. and Siesser, W. G., Cambridge University Press, Cambridge, 63–82, 1994.

Young, J. and Ziveri, P.: Calculation of coccolith volume and its use in calibration of carbonate flux estimates, Deep-Sea Res., 47, 1679–1700, 2000.

Yu, J., Broecker, W. S., Elderfield, H., Jin, Z., McManus, J., and Zhang, F.: Loss of Carbon from the Deep Sea Since the Last Glacial Maximum, Science, 330, 1084–1087, 2010.

Zeebe, R. and Wolf-Gladrow, D.: CO_2 in Seawater: Equilibrium, Kinetics, Isotopes, Elsev. Oceanogr. Series, 65, Elsevier, 2001.

Ziveri, P., Rutten, A., de Lange, G. J., Thomson, J., and Corselli, C.: Present-day coccolith fluxes recorded in central eastern Mediterranean sediment traps and surface sediments, Palaeogeogr. Palaeocl., 158, 175–195, 2000.

Ziveri, P., Baumann, K.-H., Boeckel, B., Bollmann, J., and Young, J.: Present day coccolithophore biogeography in the Atlantic Ocean, in: Coccolithophores: From Molecular Processes to Global Impact, edited by: Thierstein, H. and Young, J., Springer Verlag, 403–428, 2004.